JOURNAL OF MATERIALS SCIENCE 27 (1992) 2525–2533

# Mechanism of sintering between polypropylene beads

P. R. HORNSBY, A. S. MAXWELL
*Department of Materials Technology, Brunel University, Uxbridge, Middlesex UB8 3PH, UK*

Using experimental results obtained by hot-stage light microscopy, the sintering behaviour of off-reactor spherical grades of polypropylene and poly(methyl methacrylate) were considered. Sintering rates were found to be strongly influenced by initial particle size, melt temperature and viscosity and could be modelled using the Frenkel equation. Examination of the microstructure between sintered polypropylene particles revealed a distinct transcrystalline zone, which was relatively insensitive to sintering temperature and cooling rate.

## 1. Introduction

### 1.1. General information

Sintering is a term commonly used to describe coalescence of solid powder particles at elevated temperatures and comprises three principal stages; neck growth (joining particles together), densification, with the formation of interconnecting pore channels, followed by spheroidal shaping and isolation of pores [1]. These stages of sintering result in bonding together of particles and ultimately, to removal of internal porosity, causing external shrinkage and achievement of desirable physical properties.

Sintering processes are of major importance in powder metallurgy and in the processing of ceramics, and consequently have been the subject of considerable research effort [1–3]. Although less significant than melt processing of polymers by extrusion and injection moulding technologies, polymer sintering has an important role to play in the fabrication of artefacts, for example, by rotational moulding and fluidized-bed coating. Special processes have been developed for producing porous and densified products by sintering techniques, especially with polymers such as poly(tetrafluoroethylene) (PTFE) and ultra-high molecular weight polyethylene (UHMWPE), which are difficult to process by conventional melt-conversion procedures.

During sintering, there is a thermodynamic driving force for powders to move to a lower energy state by reducing their surface energy [4]. Kinetic factors are also important, because for sintering to proceed, atoms must have sufficient mobility to move to new positions, which, in turn, is dependent on sintering temperature.

Mechanisms by which particles may unite and coalesce during sintering vary according to the material type and conditions of sintering, but include; evaporation and recondensation, atomic diffusion at the surface or in the bulk of the material, plastic flow by dislocation movement in crystalline materials, and viscous flow [3]. More than one of these mechanisms may operate in sintering at the same time and the dominant mechanism may change during the sintering process. With polymers, however, only the viscous flow mechanism is considered to be of any major significance [5].

Although the mechanisms which operate during sintering may depend on material type, studies using spherical particles have enabled development of a common model [1]

$$\left(\frac{x}{a}\right)^n = \frac{Kt}{a^m} \tag{1}$$

where $a$ is the particle radius, $n$ the neck radius, $t$ the sintering time and $K$ a temperature-dependent constant. The magnitude of exponents $n$ and $m$ relate to the dominant mechanisms operating and may be summarized as in Table I.

### 1.2. Polymer sintering

Polymer particles, which are in contact with each other at temperatures above their glass transition or melting points, will initially form a neck, then coalesce [10]. This process occurs by movement of material from the centre of the contact region radially outwards to expand the neck between the two particles. This is believed to occur by a viscous flow mechanism in the contact zone [11, 12] with tensile capillary forces operating in the neck region [5].

The expression formulated by Frenkel [6], for prediction of viscous sintering with glasses, serves as a basis for modelling polymer sintering

$$\frac{x^2}{a} = \frac{3\upsilon t}{2\eta} \tag{2}$$

where $\upsilon$ is the surface tension and $\eta$ is the melt viscosity. This model assumes that coalescence occurs by mutual penetration of the particles into one another forming a sharp neck at the point of contact, and that in order for the volume of the two incompressible particles to remain constant, the radius of the particles is increased. Because this limits the model to the early

0022–2461  

TABLE I Exponents associated with principal sintering mechanisms [6–9]

| | $n$ | $m$ |
|---|---|---|
| Viscous or plastic flow | 2 | 1 |
| Evaporation/condensation | 3 | 2 |
| Bulk diffusion | 5 | 3 |
| Surface diffusion | 7 | 4 |

stages of sintering, a correction has been proposed [11], which considers the formation of a rounded neck and maintains constant particle volume and radius, as is observed experimentally.

Other modifications to Frenkel's model include the incorporation of a term describing a four-element Maxwell–Voigt model to account for polymer viscoelasticity [13] and adjustments to take account of possible non-Newtonian polymer melt flow. However, in several investigations using poly(methyl methacrylate) (PMMA) beads, Rosenzweig and Narkis [15] detailed improved procedures for the analysis of sintering between two connected particles and concluded that the mechanism of sintering was essentially Newtonian in accordance with Frenkel's model.

A study of polymer sintering behaviour is complicated by the presence of ordered polymer morphology. Several studies [16, 17] have shown that with semi-crystalline polymers, the internal morphology of a particle plays an even more important role than just its size. With ultra-high molecular weight polyethylene (UHMWPE), particles were considered to be aggregates of small nodules of less than 1 μm diameter and the size of these nodules was thought to influence markedly the overall sintering process. Sintering rates were also enhanced by the presence of an internal fibrillar microstructure, which increased the number of inter-particle contact points. More recently, other workers [18] have also concluded that certain semi-crystalline polyethylenes with highly developed internal morphology gave unpredictably fast rates of sintering due to their higher surface energy. Analysis of sintering behaviour could not be accounted for using existing sintering models.

The results presented here extend the work previously reported, by considering the mechanics of sintering between polypropylene beads, which are produced in spherical form by the method of polymerization. Being semi-crystalline, the microstructures produced during sintering are also of interest and receive special consideration.

## 2. Experimental procedure

### 2.1. Materials

Different grades of Valtec polypropylene homopolymer and copolymer with a range of molecular weights, were selected for this investigation (Table II). Conveniently, these are produced in approximately spherical form using special catalyst technology, facilitating study of their sintering kinetics.

As mentioned earlier, much of the previously reported work describing the sintering behaviour of polymers has been undertaken using poly(methyl methacrylate) beads. Hence, Diakon PMMA powder was included in this work to provide comparison with results obtained from polypropylene.

The microstructure at the interface between sintered spherical polypropylene beads, was also compared with that obtained using polypropylene homopolymer particles (Propathene GSE 16) obtained by knife milling extruded granules.

### 2.2. Sintering procedures

Sintering analysis was undertaken on a Reichert hot-stage microscope fitted with a 10 μm graduated eyepiece. This allowed sintering measurements to be undertaken directly from the microscope, avoiding the need to analyse micrographs in a subsequent step.

To study isothermal sintering behaviour, two similarly sized polymer particles were placed in contact on a freshly washed glass slide mounted on the microscope stage and in the centre of the field of view through the lens. (Siegmann *et al.* have shown that a glass substrate does not influence the sintering process [18].)

The cover to the hot stage was fitted and the temperature rapidly raised to the required sintering temperature. Measurements of the sintering process were taken as soon as the polymer had reached its melting point.

Neck radius was determined as a function of time, at a constant sintering temperature. This procedure was repeated for three pairs of particles from each polymer grade and at isothermal sintering temperatures of 180, 190 and 200 °C.

TABLE II Characteristics of polymers studied

| Polymer type | Shape | Code | MFI[a] (g/10 min) | Particle size (μm) (median) |
|---|---|---|---|---|
| PP homopolymer | Spherical | PP-Q | 1 | 500–1000 (750) |
| PP homopolymer | Spherical | PP-7T | 2 | 500–1000 (750) |
| PP homopolymer | Spherical | PP-T | 3 | 500–1000 (750) |
| PP homopolymer | Spherical | PP-F | 12 | 500–1000 (750) |
| PP copolymer[b] | Spherical | PP-EPT | 3 | 500–1000 (750) |
| PP homopolymer | Irregular chips | GSE16 | 0.8 | 400–800 |
| PMMA | Spherical | PMMA | | |

[a] Measured at 230° C using 2.16 kg load.

[b] Heterophase ethylene–propylene block copolymer with 7%–9% ethylene content.

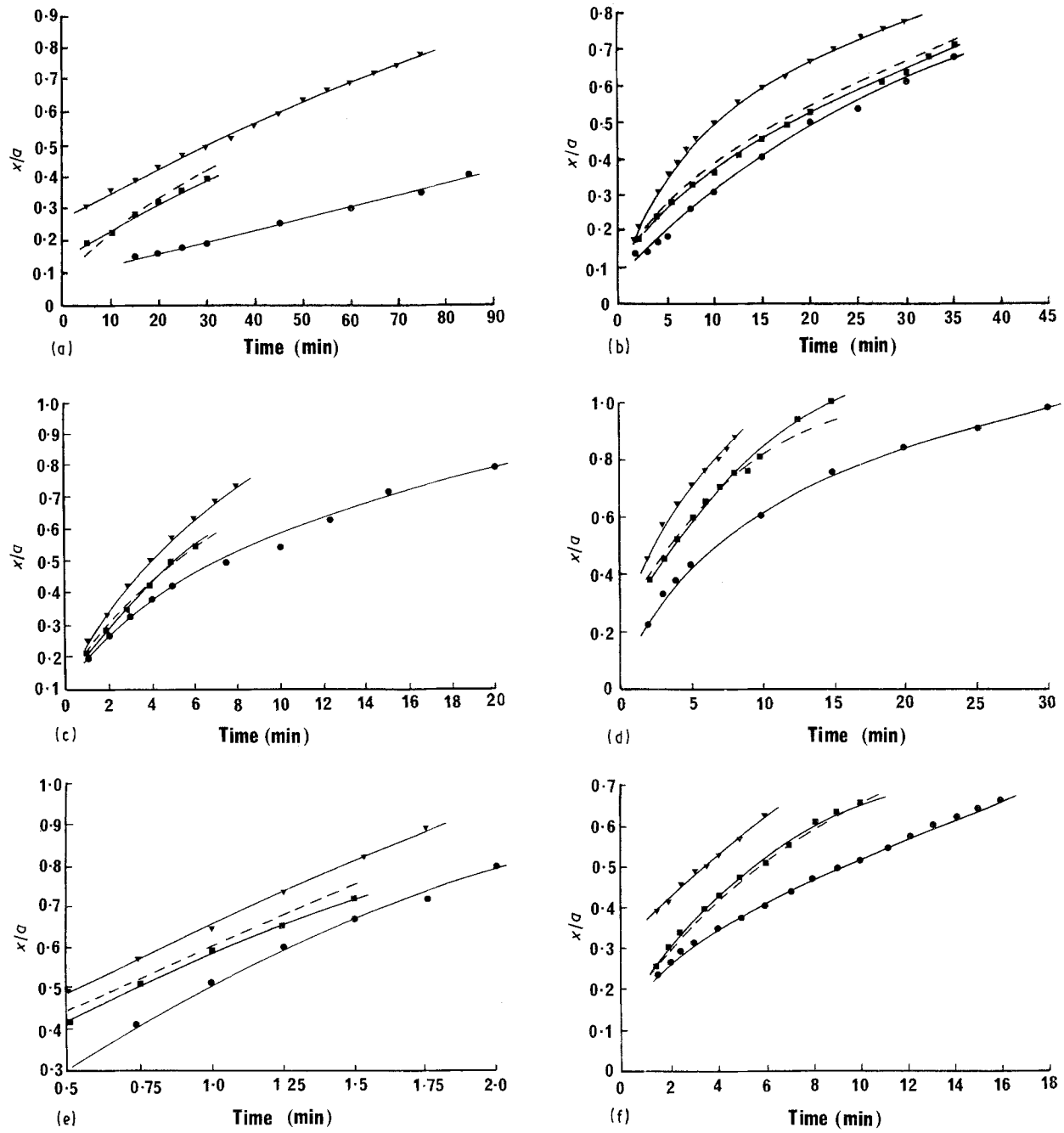


*Figure 1* The influence of temperature on the rate of neck formation between sintered polymer particles. (——) Experimental results, (– – –) predicted results using Frenkel equation. (▼) 200 °C, (■) 190 °C, (●) 180 °C. (a) PMMA, (b) PP-Q, (c) PP-7T, (d) PP-T, (e) PP-F, (f) PP-EPT.

The relative effects of initial particle size and melt viscosity on sintering kinetics, were also assessed at 190 °C, by maintaining one of these parameters constant and varying the other.

## 2.3. Polymer melt rheology

Melt viscosity data were measured at 190 °C using a Rosand capillary rhéometer using long and short dies over a shear rate range of 90–1500 $s^{-1}$. Values for apparent shear viscosity were corrected for end effects and extrapolated to yield a shear viscosity at a shear rate of 0.3 $s^{-1}$. This value was used in the modelling of sintering kinetics.

## 2.4. Interparticle morphology

Sintered polypropylene particles were prepared at constant temperatures of 180 and 200 °C until the neck radius was approximately equal to the particle radius. Samples produced at these temperatures were quenched from the sintering temperature in a water/ice mixture at 0 °C and by slow cooling in air. In addition, the microstructure of the unsintered polymer particles was also examined.

From each of the prepared samples, microtomed sections (approximately 5 μm thick) were obtained using a sledge cold-stage microtome. To facilitate specimen preparation, sintered particles were placed on top of an ice layer on the cold stage then covered in water to encase them in ice. By this means, the speed of preparing sections was greatly increased, compared to more conventional resin encapsulation methods, and good control of the specimen positioning was obtained. Microtomed sections were taken at various levels through the specimen thickness and across the

interparticle neck region, then examined under a Reichert-Jung Microstart 110 microscope using crossed polars.

## 3. Results and discussion

### 3.1. Kinetics and mechanisms of sintering

Isothermal sintering results for the spherical polypropylene and poly(methyl methacrylate) particles are shown in Fig. 1a–f, as the relationship between $x/a$ (the ratio of interparticle neck to particle radius) and $t$ (the sintering time). The curved form of these graphs is consistent with sintering data reported for many other materials. The progressive decrease in sintering rate observed, is due to the reduction in excess surface area effected as the sintering process progresses [4].

As might be expected, raising the sintering temperature results in an increase in the rate of sintering, due to greater molecular mobility and increased material transport in the sintering zone.

The assumption that the flow in polymer sintering is Newtonian was made by Narkis [14], who argued that although polymers generally exhibit pseudoplastic melt flow, during polymer sintering shear rates are so low that flow remains Newtonian.

Kuczynski *et al.* [5], however, proposed a relationship based on power law flow to describe polymer sintering phenomena

$$\left(\frac{x^2}{a}\right)^n = K(T)t \tag{3}$$

where $n$ is a temperature-dependent constant, which varies according to the melt flow behaviour, from dilatent at low temperatures to pseudoplastic at higher temperatures.

To assess whether or not melt viscosity in the present study was Newtonian, the relationship between log $x/a$ and log viscosity is given in Fig. 2. Elongational viscosity data are presented, calculated from shear viscosity data (as explained later), because this is believed to be the predominant form of melt flow during sintering. The gradient obtained from a linear regression analysis of these data gave a value of $-0.48$ verifying the Frenkel model, and confirming that the melt flow during the sintering process was Newtonian.

Initial particle size is also considered to be a critical parameter in polymer sintering. For example, Jayaraman *et al.* [19] concluded that by using smaller particles the sintering rate could be increased. To assess the effect of polypropylene particle size on sintering kinetics, experiments were undertaken on Q grade beads, varying in radius from 430–380 μm. The extent of neck formation (log $x/a$) is related to initial particle size (log $a$) in Fig. 3. The gradient of this curve is calculated as $-0.45$ which again closely approximates Frenkel's theoretical relationship, i.e.

$$\frac{x}{a} \propto 1/a^{1/2} \tag{4}$$

This derives from the fact that the smaller the particle size the greater its surface area and thermodynamic driving force, thereby increasing the rate of sintering.

Representation of the experimental data, as the relationship between log $(x/a)^2$ and log $t$, is shown for the polymer grades studied in Fig. 4 at three different sintering temperatures. Using a least squares regression analysis, gradients were determined, which are summarized in Table III. These are very close to a theoretical value of 1, which would be the case for polymer sintering by a viscous flow mechanism. This contrasts with values of between 0.5 and 5 obtained by Kuczynski *et al.* [5] using PMMA over a wider temperature range than that employed in the present study and between 0.89 and 1.82, found by Narkis [14], again using PMMA.

Calculated polymer sintering rates at 190 °C were determined using the Frenkel equation (Equation 2) with the following assumptions:

(i) particles were considered to be of an equal size and perfectly spherical;

(ii) the value of surface tension, υ, was taken as 34 mN m$^{-1}$, as has been reported previously [17, 20];

(iii) all sintering stresses were considered to be tensile [5, 21].

To obtain elongational viscosity data for use in this model, values of Trouton viscosity were calculated from the experimentally determined shear viscosity data extrapolated to give a value of apparent viscosity at a shear rate of 0.3 s$^{-1}$ following recommendations from previously published work [18]. Assuming melt incompressibility and a Poisson's ratio of 0.5, Trouton

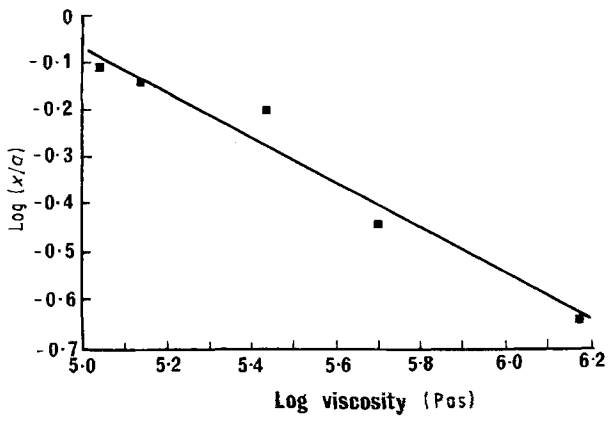


*Figure 2* The effect of melt viscosity on degree of sinter with polypropylene beads.

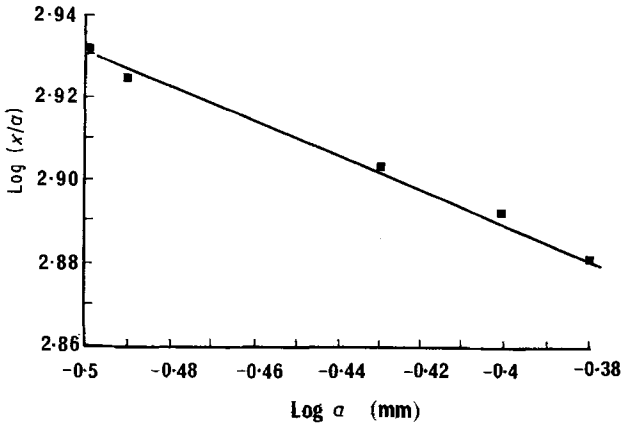


*Figure 3* The effect of particle size on the degree of sinter with polypropylene beads.

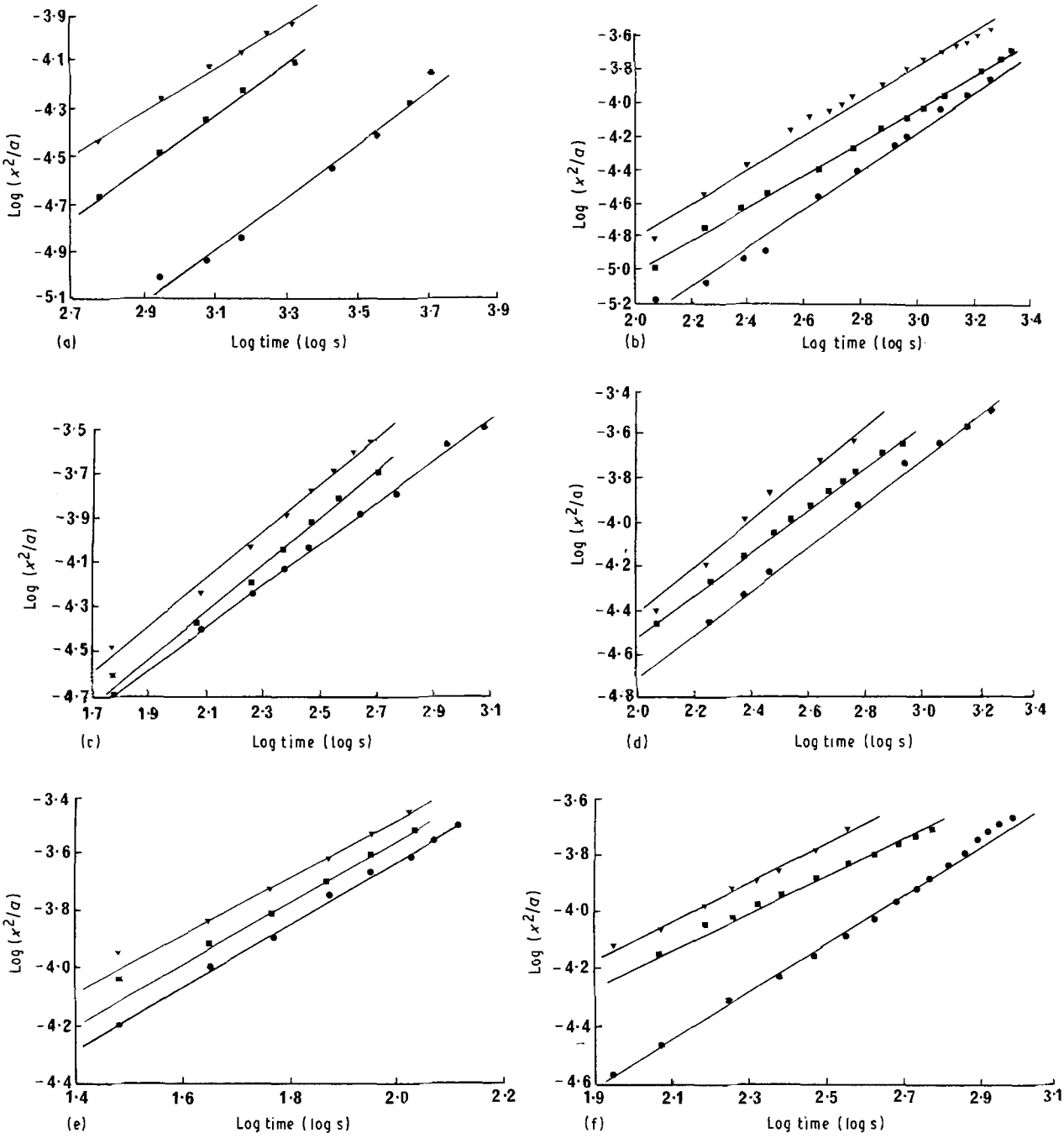


*Figure 4* Logarithmic rates of neck formation between sintered polymer particles. (▼) 200 °C, (●) 180 °C, (■) 190 °C. (a) PMMA, (b) PP-Q, (c) PP-7T, (d) PP-T, (e) PP-F, (f) PP-EPT.

viscosities were calculated from three times the apparent shear viscosity [22].

Good agreement is seen between predicted and experimentally determined rates of sintering for all of the polymers studied (Fig. 1).

TABLE III Gradients of log ($x^2/a$) plotted against log time

| Polymer grade | Sintering temperature (°C) | | |
|---|---|---|---|
| | 180 | 190 | 200 |
| Q | 1.17 | 1.02 | 1.06 |
| 7T | 0.95 | 1.15 | 1.07 |
| T | 0.99 | 0.96 | 1.06 |
| F | 1.07 | 1.05 | 0.98 |
| EPT | 0.98 | 0.80 | 0.83 |

## 3.2. Microstructure

It has been observed that certain semi-crystalline polymers sinter at unexpectedly fast rates, due to their highly developed internal morphology and increased surface energy [18]. However, as discussed earlier, the spherical forms of polypropylene used in this work followed a classical sintering mechanism. Microtomed sections of the unsintered polymer viewed under crossed polars, revealed only limited or partial development of crystalline morphology (Fig. 5), which presumably had little influence on the sintering kinetics. It is apparent from Fig. 6 that at low sintering temperatures (180 °C), the lack of organized structure evident in unsintered polymer was to some extent seen in sintered material (see, for example, Fig. 6d) although in most cases a more fully developed microstructure had resulted.

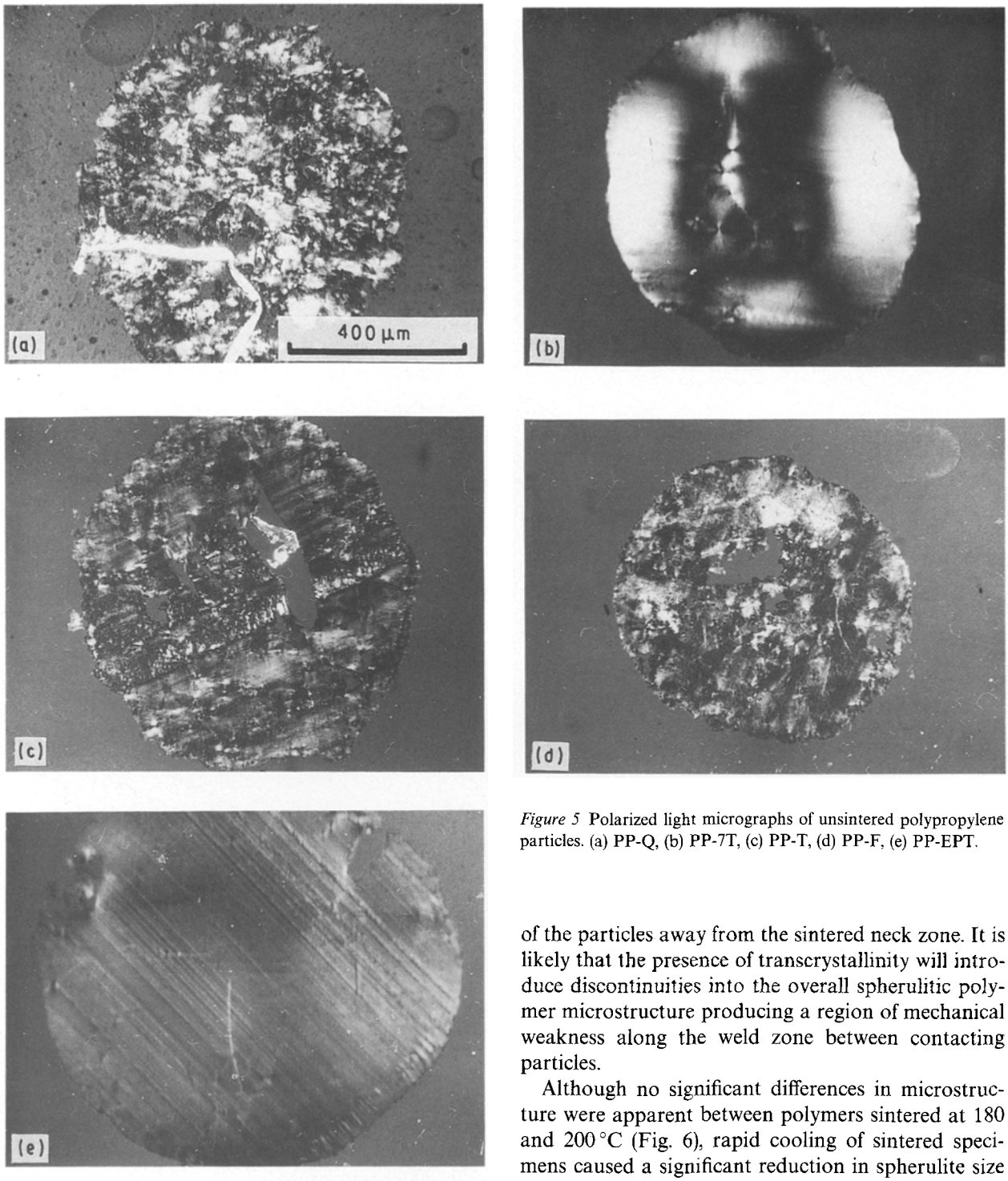


*Figure 5* Polarized light micrographs of unsintered polypropylene particles. (a) PP-Q, (b) PP-7T, (c) PP-T, (d) PP-F, (e) PP-EPT.

The reduced structural order present in this form of unsintered polypropylene, compared to conventional pellets is claimed to give easier melting and increased productivity in melt-processing operations [23]. It may also influence the sintering kinetics, because the polymer may exhibit characteristics closer to an amorphous rather than a semi-crystalline polymer.

Of particular interest, is the nature of the microstructure at the interface between sintered particles (Fig. 6). Whereas the spherulitic growth within the particles appeared uniform and isotropic, at the point of contact between sintered particles a distinct transcrystalline columnar structure is apparent. This form of morphology can also be seen around the periphery of the particles away from the sintered neck zone. It is likely that the presence of transcrystallinity will introduce discontinuities into the overall spherulitic polymer microstructure producing a region of mechanical weakness along the weld zone between contacting particles.

Although no significant differences in microstructure were apparent between polymers sintered at 180 and 200 °C (Fig. 6), rapid cooling of sintered specimens caused a significant reduction in spherulite size and a corresponding decrease in the depth of the transcrystalline layer (Fig. 7). It was thought possible that stabilizer added to the surface of the polypropylene particles after polymerization, may have resulted in surface nucleation and the formation of the observed transcrystalline zone. Sintering experiments were conducted, therefore, on size-reduced polypropylene granules made by an extrusion process and containing well-distributed stabilizer particles. However, as can be seen in Fig. 8, a clear zone of transcrystallinity is again dominant at the interface between sintered particles, from this material.

It has been reported that during viscous sintering between polymer particles, tensile capillary forces are developed which cause the polymer to flow outwards from the centre of the neck [11, 21]. To verify this phenomenon with polypropylene beads used in this

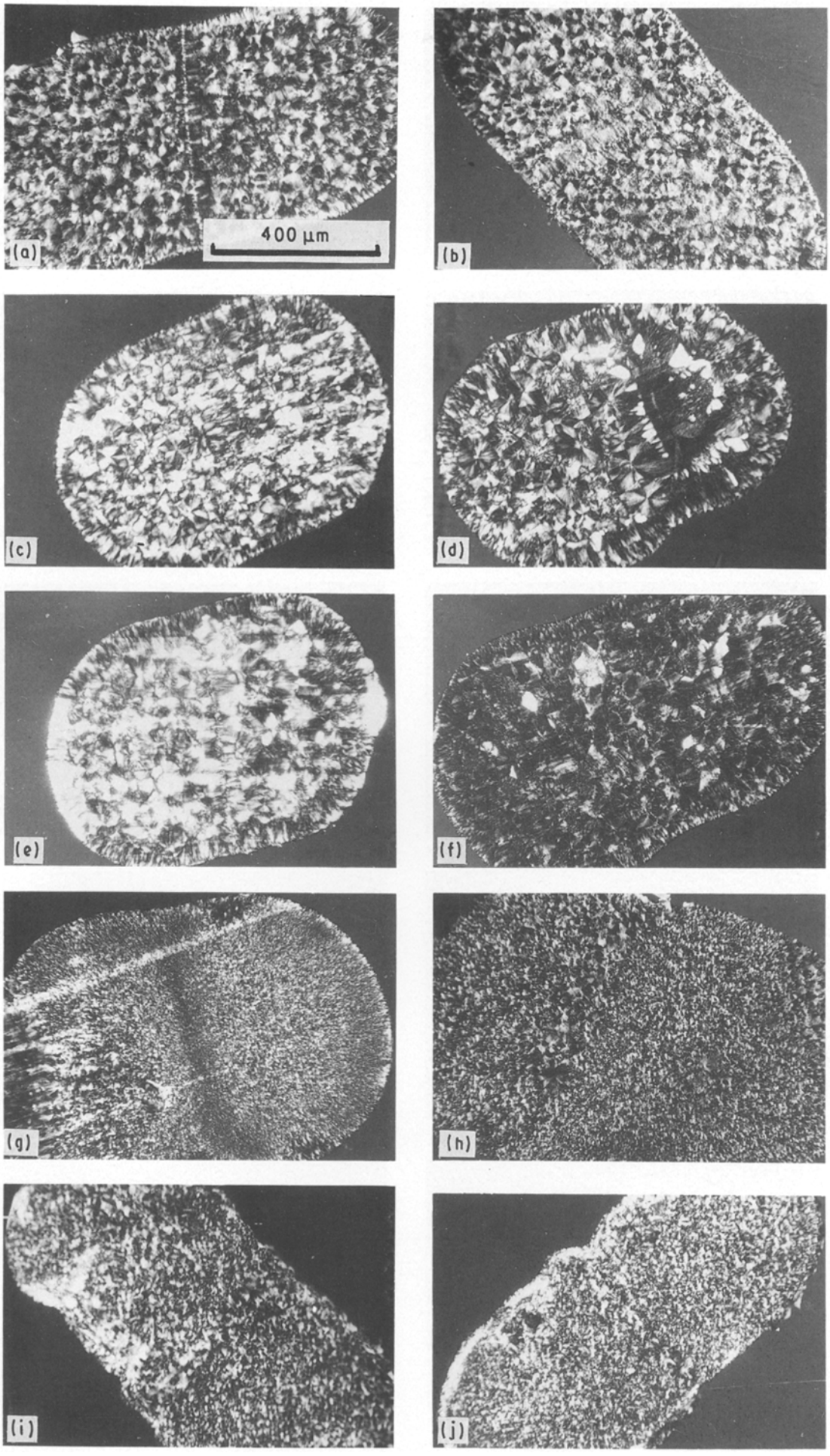


*Figure 6* The influence of sintering temperature on the microstructures of polypropylene particles. (a, b) PP-Q, (c, d) PP-7T, (e, f) PP-T, (g, h) PP-F, (i, j) PP-EPT. (a, c, e, g, i) 200 °C; (b, d, f, h, j) 180 °C.

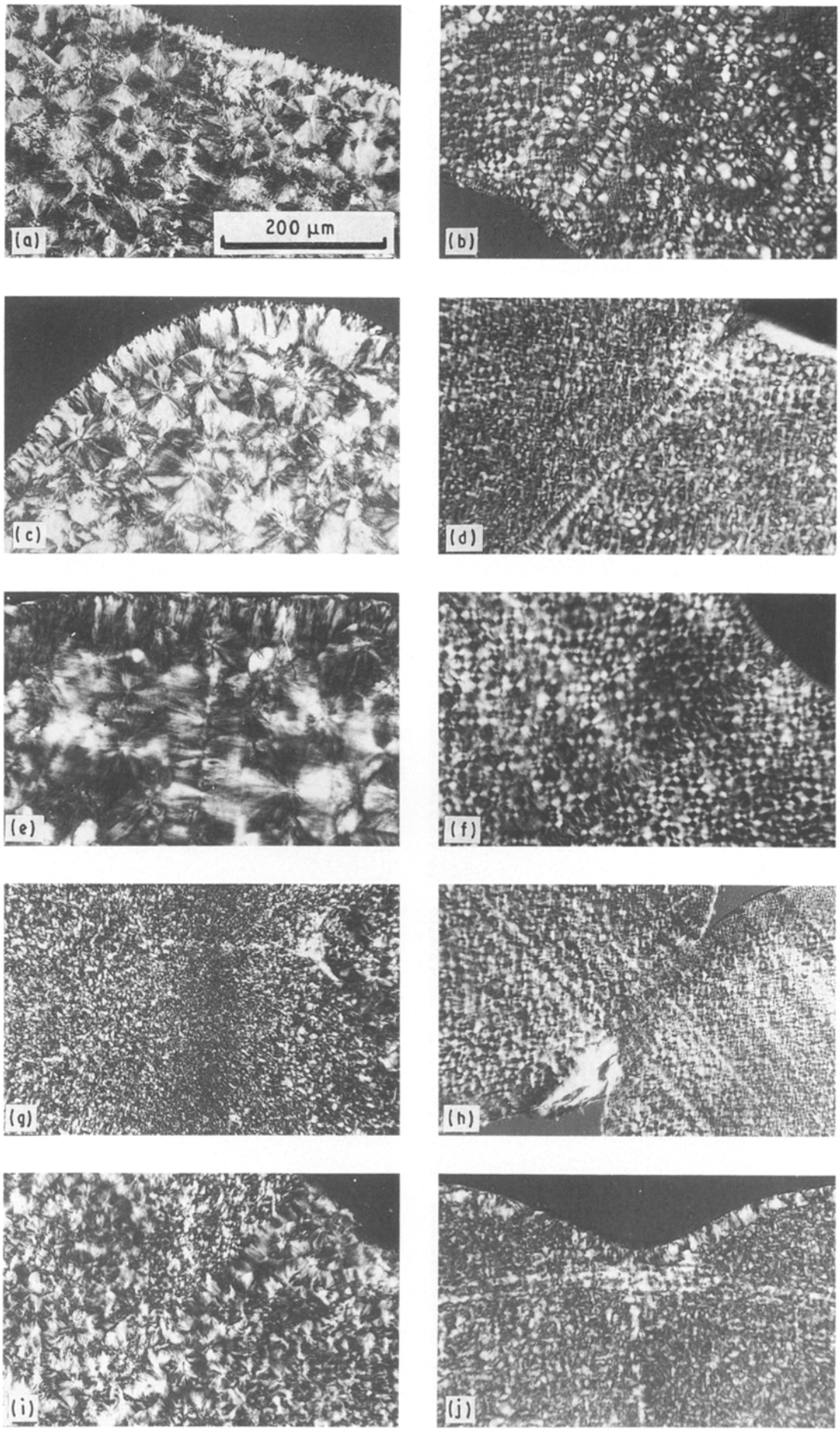


*Figure 7* The effect of cooling rate on the microstructure of sintered polypropylene particles. (a, b) PP-Q, (c, d) PP-7T, (e, f) PP-T, (g, h) PP-F (i, j) PP-EPT. (a, c, e, g, i) 25 °C air; (b, d, f, h, j) 0 °C, ice/water.

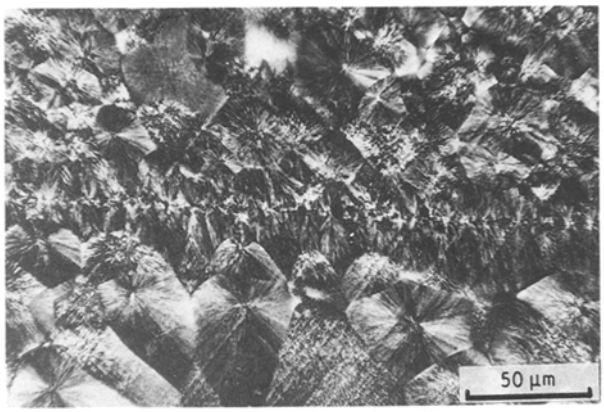


*Figure 8* Later-particle microstructure of sintered Propathene GSE 16 polypropylene.

study, a tracer experiment was undertaken, in which a small quantity of blue dye was placed at the point of contact between two polymer particles. As sintering proceeded the tracer was seen to spread outwards along the weld line as neck formation developed. Microscopic examination of microtomed sections through this area, showed that the dye tracer was distributed across the whole of the interfacial zone and at the centre of the transcrystalline region between the particles.

## 4. Conclusions

Reproducible analysis of sintering rates between polypropylene particles can be undertaken by direct measurements on a hot-stage microscope.

Both spherical off-reactor grades of polypropylene and PMMA beads heated to temperatures between 180 and 200 °C, sintered by a viscous Newtonian flow mechanism.

Good agreement was seen between experimental results for polypropylene obtained at 190 °C and predicted sintering rates using the classical Frenkel model, as has been previously reported for amorphous PMMA, but in contrast with the results for certain semi-crystalline polymers, including polypropylene. This may be due to the apparent lack of structural order seen in the unsintered off-reactor polypropylene beads used in this study. Changing the particle size and melt viscosity of this material also gave sintering rates which agreed well with the Frenkel model.

Distinct zones of transcrystallinity were seen at the interface between sintered polypropylene particles, and cooling rate did not significantly affect the formation of transcrystallinity, although rapid quenching reduced the average size of the spherulites by an order of magnitude. The cause of this mass nucleation, resulting in transcrystalline growth could not be attributed to the presence of polymer stabilizer believed to be situated at the surface of the particles.

Using a tracer technique, contacting polypropylene particles were observed to flow radially outwards from the centre of the neck.

## Acknowledgements

The authors are grateful to Himont (Italy) and Sinterform Ltd for provision of materials used in this study.

## References

1. F. THUMMLER and W. THOMMA, *Met. Rev.* **12** (1967) 69.
2. R. L. COBLE and J. E. BURKE, *Prog. Ceram. Sci.* **3** (1963) 197.
3. A. J. ALLER, *Cerm. Ind. J.* August (1986) 39.
4. A. J. SHALER, *AIME Met. Trans.* **18** (1949) 796.
5. G. C. KUCZYNSKI, B. NEVILLE and H. P. TONER, *J. App. Polym. Sci.* **14** (1970) 2069.
6. J. FRENKEL, *J. Phys. (USSR)* **9** (1945) 385.
7. G. C. KUCZYNSKI, "Theory of solid state sintering" in Powder Meltallurgy, edited by W. Leszynski (Interscience, 1961).
8. W. D. KINGERY and M. BERG, *J. Appl. Phys.* **26** (1955) 1205.
9. C. HERRING, *J. Appl. Phys.* **21** (1950) 301.
10. Z. TADMOR and G. C. GOGOS, "Principles of Polymer Processing" (Wiley Interscience, 1979).
11. N. ROSENZWEIG and M. NARKIS, *Polymer* **21** (1980) 988.
12. *Idem., Polym. Engng Sci.* **21** (1981) 582.
13. I. F. LONTZ, "Fundamental phenomena in the material sciences", Vol. 1 (Plenum Press, 1964).
14. M. NARKIS, *Polym. Engng Sci.* **19** (1979) 889.
15. N. ROSENZWEIG and M. NARKIS, *J. Appl. Polym. Sci.* **26** (1981) 2787.
16. G. W. HALDIN and I. L. KAMEL, *Poly. Engng Sci.* **17** (1977) 21.
17. R. W. TRUSS, *ibid.* **20** (1980) 747.
18. A. SIEGMANN, I. RAITER and P. EYERER, *J. Mater. Sci.* **21** (1986) 1180.
19. G. S. JAYARAMAN, J. F. WALLACE, P. H. GEIL and E. BAER, *Polym. Engng Sci.* **16** (1976) 529.
20. D. W. VAN KREVELEN, "Properties of Polymers" (Elsevier, 1976).
21. R. L. SANDS and C. R. SHAKESPEARE, "Powder Metallurgy" (Newnes, London, 1966).
22. J. A. BRYDSON, "Flow properties of polymer melts", 2nd Edn (George Godwin, 1981).
23. Anon, *Plast. Rubber Int.* **14** (1989) 4.

*Received 21 January*
*and accepted 7 June 1991*